Journal of Engineering Mathematics **33:** 15–30, 1998.

Contamination pattern in groundwater resulting from an underground source

ARIEH PISTINER[1] and MICHAEL SHAPIRO[2]
[1]*Ministry of Environment, Water Quality Division, 2 Chury St., Haifa 33045, Israel*
[2]*Faculty of Mechanical Engineering, Technion-Israel Institute of Technology, Haifa 32000, Israel*

Received 25 July 1995; accepted in revised form 25 April 1997

Abstract. Steady distribution of oil pollutant within an aquifer, discharging from an underground source, is modeled by a two-dimensional nonlinear diffusion-convection equation. This equation describes oil transport in the immiscible zone, containing large oil blobs. This zone serves as a secondary source of contaminant in the dispersed zone, containing freely flowing oil drops. A self-similar solution is obtained for the steady saturation distribution in the immiscible zone, which is valid at distances greatly exceeding the source size across the water-flow direction.

The distribution of oil saturation within the aquifer is investigated numerically and analytically as a function of the water-flow rate, pore sizes and the leakage rate of the oil-pollution source. This rate is characterized by a dimensionless parameter, dependent on the oil viscosity, aquifer permeability and the water-flow rate in the aquifer. Various flow regimes are described which yield plum-like contamination patterns. The location of the boundary between the immiscible and dispersed oil zones is calculated in terms of the source-strength parameter, water and oil properties and porous-medium structure. A closed form analytical solution is obtained in a particular case where a linear relationship exists between parameters governing advection and dispersion oil-transport rates.

Key words: aquifer, oil saturation, pollution, self-similar solution, groundwater.

1. Introduction

Transport of pollutants in groundwater flows is an important engineering and environmental problem. Groundwater contamination may result from contaminant leakages from various sources, including storage tanks, pipelines, etc. This study is devoted to investigation of the contamination pattern which may result from such leakages.

Various experimental studies [1] reveal that oil contained in a porous medium, fully saturated with water, (*e.g.*, a saturated aquifer) is partitioned between two zones: The first is the immiscible zone, containing mostly oil blobs, which are normally larger than the average pore size and held in pore spaces by the capillary forces. The extension of the immiscible zone depends on the strength of the capillary forces, which is inversely proportional to the pore size. This zone is larger in porous media containing finer pores [2].

Adjacent to the immiscible zone is the dispersion zone, containing oil drops which are much smaller than the pore size. The oil blobs present in the immiscible zone constitute obstacles to the water flow. On the contrary, in the dispersion zone, the oil-water emulsion flows freely within the aquifer according to the mass transport advection-dispersion laws [3, pp. 457–468]. The oil blobs present in the immiscible zone serve as sources for contamination of the dispersion zone. Field studies of oil transport processes show [4] that the contaminant distributes in the aquifer between the two zones, as described above.

Here we treat the problem of contamination of an aquifer, resulting from a continuously leaking source by modeling oil exchange between the immiscible and dispersed zones. The goal of this work is the determination of the extension of the immiscible zone for different flow conditions.

Several models have been developed which are aimed at describing the oil-transfer process between the two zones. Spielman and Su [5] assumed that the oil-transfer rate between these zones depends on the droplet size, local flow rate, surface-tension parameters, chemical environment and the local geometry of the porous medium. Spielman and Goren [6] treated the problem of oil transfer between the two zones by assuming that blobs held by the capillary forces in the porous medium form a network of channels. These channels are sufficiently well connected to enable viscous oil flow. The oil in the immiscible zone prevails in a local equilibrium with the solid and water phase in accordance with the surface tension coefficients governing capillary pressure. When the blobs held in the pores are much larger than the average pore size, large local water-pressure gradients force the trapped blobs through the pores, thereby causing transport of the trapped oil. This process is accompanied by irreversible rupture of the transported blobs with subsequent formation of small droplets, which are further transported in the dispersed zone.

Determination of the extension of the immiscible zone is important for various practical purposes. This is characterized in terms of the oil saturation S, defined as volumetric fraction occupied by the oil in a porous medium fully saturated with oil-water mixture. Pinder and Abriola [7] calculated numerically evolution of the two-dimensional oil distribution in the immiscible zone by assuming the iso-saturation line $S = 0{\cdot}1$ in the immiscible zone to be a surface source of the dissolved oil in the dispersion zone.

In various hydrological applications the inverse problem of groundwater contamination is of crucial importance. It means that field data taken in several observation wells are used to assess the global extension of the contamination, locate its source and evaluate the evolution of the contamination pattern for given ground-water flow conditions. For this purpose a simple model is needed, which enables evaluation of the influence of the oil-discharge rate, groundwater flow rate, oil-water properties and porous structure of the aquifer on the extension of the immiscible zone. This work is devoted to the above purpose. We use the equations of two-phase oil-water transport in the immiscible zone to calculate the steady-state oil distribution, and, in particular, the location of the boundary between the immiscible and the dispersed zones.

The paper is constructed as follows: The second and the third sections deal with the physico-mathematical model, basic assumptions and problem formulation. In the fourth section the general similarity solution is developed, which allows reduction of the problem to the solution of ODEs. These were solved numerically and also analytically in a particular case where a closed-form solution exists. Section five is devoted to analysis and discussion of the results.

2. Physico-mathematical model

Consider a two-dimensional homogeneous, generally anisotropic horizontal porous layer (of an aquifer) fully saturated with water, on the regional scale, *i.e.*, over a planar horizontal extent much larger than its thickness. Consider also a line source of oil of size L^* located in the layer, (see Figure 1) which discharges oil with a constant volumetric rate $\dot{Q}^*$. It is assumed that there is a water flow in the positive y-direction within the aquifer.

We will refer to L^* as the length of the source perpendicular to the average water-flow direction. The extension of the source along the flow is unimportant since the solution to be developed will be shown to be valid far downstream from the source. In this situation we will

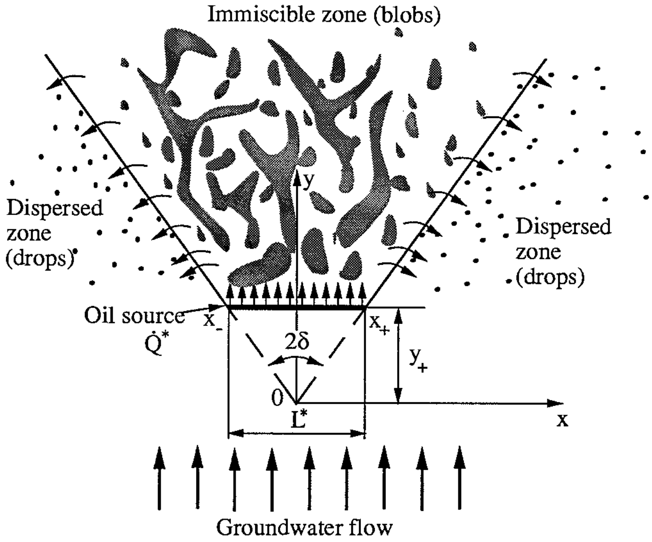

Figure 1. Schematic description of two-dimensional flow of oil-water mixture in the aquifer resulting from an oil source.

show that it is the length of the line source in the x-direction and the total discharge $\dot{Q}^*$ which in fact affect the oil-saturation distribution.

The respective specific discharge vectors $\mathbf{q}_w$ and $\mathbf{q}_o$ of the water and the oil in the immiscible zone in the absence of the gravity force, are modeled by Darcy's law. We can write this for each fluid in a Cartesian system, using the double index summation convention $(x_1 = x, x_2 = y)$ in the form

$$q_{w_i} = -\kappa_{ij} \frac{K_{rw}(S)}{\mu_w} \frac{\partial P_w}{\partial x_j}, \quad i = 1, 2 \tag{1}$$

and

$$q_{o_i} = -\kappa_{ij} \frac{K_{ro}(S)}{\mu_o} \frac{\partial P_o}{\partial x_j}, \quad i = 1, 2, \tag{2}$$

where S is the macroscopic (averaged over the layer height) oil saturation in the immiscible zone $(0 < S < 1)$; $K_{rw}(S), K_{ro}(S)$ are the relative permeabilities, dependent only on the oil saturation. Other quantities appearing in (1), (2) are: κ_{ij} – the Cartesian components of the permeability tensor, μ_o, μ_w – the oil and water viscosities, respectively, P_o, P_w – the oil and water pressures respectively, which are related via the capillary pressure P_c

$$P_c(S) = P_o - P_w. \tag{3}$$

The conservation of mass for each fluid in a rigid porous medium of porosity ϕ yields

$$\frac{\partial q_{w_i}}{\partial x_i} - \phi \frac{\partial S}{\partial t} = 0, \quad i = 1, 2 \tag{4}$$

and

$$\frac{\partial q_{o_i}}{\partial x_i} + \phi \frac{\partial S}{\partial t} = 0, \quad i = 1, 2, \tag{5}$$

where t is the time variable. Combining (1)–(5), we obtain [2]

$$\phi\frac{\partial S}{\partial t} = \frac{\partial}{\partial x_i}\left(\Psi(S)\kappa_{ij}\frac{\partial S}{\partial x_j} - q_i F(S)\right), \tag{6}$$

where

$$q_i = q_{w_i} + q_{o_i}, \quad i = 1, 2 \tag{7a}$$

and

$$F(S) = \left[1 + \frac{K_{rw}(S)\mu_o}{K_{ro}(S)\mu_w}\right]^{-1}, \quad \Psi(S) = \frac{K_{rw}(S)}{\mu_w}\frac{\mathrm{d}P_c(S)}{\mathrm{d}S}F(S). \tag{7b, c}$$

Adding Equations (5) $(i = 1, 2)$, we obtain

$$\frac{\partial q_i}{\partial x_i} = 0.$$

We will further assume that the flow is unidirectional. Thus, from the above equation we obtain $q_y = q, q_x = 0$. Generally, the total discharge q can depend on time (*e.g.*, as a result of rains). We will assume here $q =$ constant, which is known for given aquifer conditions. In addition we will set [3] $\kappa_{xy} = \kappa_{ys} = 0$. The fractional flow curve $F(S)$ and the function $\Psi(S)$ can be represented by power-law relationships [2, 8], usually valid for low oil saturation

$$F(S) \cong F_0 S^n, \quad \Psi(S) = \frac{\gamma_{ow}}{\mu_w}\Psi_0 S^{n-m}, \tag{8a, b}$$

where γ_{ow} is the oil-water surface tension coefficient. Moreover, we can deduce from (7)–(8) that F_0 is a dimensionless factor of order one, and Ψ_0 is of order $\Delta P_c/\gamma_{ow}$, where ΔP_c is a characteristic capillary pressure in the aquifer. Parameters m and n were found to depend on the oil and water properties, in particular, viscosities and also on the pore-size index of the porous medium [2]. From the experimental data on fractional flow rates and permeabilities it was found that m and n typically vary in the following ranges: $1 < n < 3, 1{\cdot}5 < m < 4$.

3. Mathematical formulation

We define dimensionless variables

$$\hat{x} = x/L_x; \quad \hat{y} = y/L_y; \quad \hat{t} = t/T, \tag{9a, b, c}$$

where the characteristic convective lengths, L_x, L_y and the characteristic convective time, T, are

$$L_x = \frac{\Psi_0\gamma_{ow}\sqrt{\kappa_{xx}\kappa_{yy}}}{qF_0\mu_w}, \quad L_y = \frac{\Psi_0\gamma_{ow}\kappa_{yy}}{qF_0\mu_w}, \quad T = \frac{L_y\phi}{qF_0}. \tag{9d, e, f}$$

Introduce (9a–f) into Equations (6), (8a, b) to obtain

$$\frac{\partial S}{\partial \hat{t}} + \frac{\partial J_x}{\partial \hat{x}} + \frac{\partial J_y}{\partial \hat{y}} = 0, \tag{10a}$$

where J_x, J_y are the dimensionless oil-flux components

$$J_x = -S^{n-m}\frac{\partial S}{\partial \hat{x}}, \quad J_y = -S^{n-m}\frac{\partial S}{\partial \hat{y}} + S^n. \tag{10b, c}$$

We will assume that a steady oil-saturation distribution is established after a sufficiently long time following the release of oil $(t \gg T)$. In such a case $\partial S/\partial \hat{t}$ on the left-hand side of (10a) vanishes and Equations (10a, b, c) describe a steady-state distribution of the oil saturation $S(\hat{x}, \hat{y})$ within the aquifer.

The volumetric discharge $\dot{Q}^*$ of the pollutant may be calculated by integration of the oil flux over the length of the source (*cf.* Equation (6))

$$\dot{Q}^* = \int_{-L^*/2}^{+L^*/2} \left[\Psi(S)\kappa_{yy}\frac{\partial S}{\partial y} - qF(S)\right]\Bigg|_{y=y+} \mathrm{d}x = \frac{\gamma_{ow}}{\mu_w}\Psi_0\sqrt{\kappa_{xx}\kappa_{yy}}\int_{-L/2}^{+L/2} J_y\Bigg|_{\hat{y}=\hat{y}+} \mathrm{d}\hat{x},$$

where y^+ is related to the position and the size of the oil source, to be specified below. This equation combined with (9b) and (10c) may be recast in the form

$$\dot{Q} = \frac{\mu_w \dot{Q}^*}{\gamma_{ow}\Psi_0\sqrt{\kappa_{xx}\kappa_{yy}}} = \int_{-L/2}^{+L/2} J_y\Bigg|_{\hat{y}=\hat{y}+} \mathrm{d}\hat{x}, \tag{11a}$$

wherein the dimensionless parameter L is defined as

$$L = L^*\frac{\mu_w q F_0}{\gamma_{ow}\Psi_0\sqrt{\kappa_{xx}\kappa_{yy}}}. \tag{11b}$$

Far from the source, where the sizes of oil blobs diminish, the oil saturation decreases down to the value $S = 0$ and the immiscible zone terminates. Beginning from this location the oil prevails only in the dispersed phase. In fact, the boundary between the immiscible zone and the dispersion zone is not clearly defined. Rather, a transition zone exists which contains oil drops of different sizes [9]. However, we will assume that the transition zone is very narrow and that immiscible and dispersion zones are separated by boundaries

$$\hat{y} = Y(\hat{x}), \quad \hat{x}_+ < \hat{x} < \infty, \tag{12a}$$

$$\hat{y} = -Y(\hat{x}), \quad -\infty < \hat{x} < \hat{x}_-, \tag{12b}$$

where $\hat{x}_\pm = \pm L/2$ in accordance with the coordinate system chosen (see Figure 1). This assumption is consistent with various field observations [7] and implies that the minimal iso-saturation line $S = 0$ serves as a boundary between the two zones. In accordance with the above, the solution for the steady-state oil saturation is subject to the following boundary conditions

$$S(\hat{x}, Y(\hat{x})) = 0, \quad \hat{x}_+ < \hat{x} < \infty, \tag{13a}$$

$$S(\hat{x}, -Y(\hat{x})) = 0, \quad -\infty < \hat{x} < \hat{x}_-. \tag{13b}$$

We will place the origin of the coordinate system at the point located at a distance $\hat{y}_+$ upstream of the leakage source. This distance is to be determined in the course of the solution process, together with the boundary separating the immiscible and the dispersion oil zones.

All iso-saturation lines are symmetrical with respect to the flow direction (*i.e.*, the $\hat{y}$ direction). Hence the problem may be posed in the domain $Y(\hat{x}) < \hat{y} < \infty, 0 < \hat{x} < \infty$, with an additional boundary condition imposed at $\hat{x} = 0$

$$\frac{\partial S}{\partial \hat{x}} = 0 \quad \text{on } \hat{x} = 0. \tag{14}$$

At early times, when the oil transport is affected by the initial saturation distribution, Equations (10a, b, c) should be solved for the function $S(\hat{x}, \hat{y}, t)$ which involves in particular, calculation of the boundary $Y(\hat{x}, t)$ separating the immiscible and dispersion oil zones (see Equations (13a, b)). This requires formulation of an additional boundary condition, expressing continuity of the oil flux across the boundary [5]. As a result, in this case the problem should be solved both in the immiscible and the dispersion zones.

We will look for a long-time solution of Equations (10a, b, c), where the saturation reaches a steady-state form $S(\hat{x}, \hat{y})$. This means that the oil discharged per unit time by the source is equal to the total oil flux across the transition zone $Y(\hat{x})$. Estimates performed in the discussion section show that such a steady saturation distribution is contaminated sand aquifers is reached after about six months. At such long times the solution in the dispersion zone is unnecessary, since both the boundary $Y(\hat{x})$ and the oil saturation $S(\hat{x}, \hat{y})$ in the immiscible zone are determined from the symmetry properties (similarity nature) of the problem. An additional boundary condition, required in order to obtain an unambiguous solution is the integral relation (11a) between the oil discharge rate and the strength $\dot{Q}$ of the oil contamination source.

In the following section we will develop a solution which is valid at large distances from the leakage place $(\hat{x}, \hat{y} \gg L)$, *i.e.*, where it may be viewed as a point source. The similarity solution developed here satisfies the integral equation (11a). In the case where the real oil-flux distribution along the line source is consistent with the solution $J_y(\hat{x}, \hat{y}_+)$ (see (39a)), the similarity solution developed in the following section is valid everywhere within the domain $|\hat{x}| > L/2, y > \hat{y}_+$.

In fact, the oil-discharge-flux distribution is generally unknown. It is the total discharge $\dot{Q}^*$ which is of interest in hydrological applications. In this case the solution obtained here is valid for large distances $\hat{y} - \hat{y}_+ \gg L$ from the source.

4. Self-similar solution

We assume that at the steady-state the distribution of the residual oil is derived from a certain universal behavior, which is investigated in this study by the similarity method. Towards this end we look for a transformation that reduces the nonlinear PDE (10a, b, c) into an ODE. Explicitly, we construct a similarity solution of the form

$$S(\hat{x}, \hat{y}) = u(\xi)^{1/(n-m+1)} \hat{y}^{1/(1-m)}, \quad \xi = \hat{x}/\hat{y}, \tag{15a, b}$$

where $u(\xi)$ is a similarity function. This implies that the boundary $Y(\hat{y})$ in Equation (12a) is a straight line $Y(\hat{x}) = \hat{x}/\xi_b$, where a constant ξ_b is to be determined. In particular, ξ_b satisfies the relation

$$L/2 = \xi_b \hat{y}_+. \tag{15c}$$

Substituting (15a, b) in (10a, b, c), we obtain

$$\frac{u'(1+\xi^2)}{n-m+1} = g(\xi) - \xi u^{n/(n-m+1)} - \frac{2}{m-1}u\xi, \tag{16a}$$

$$g' = \frac{n-m+1}{m-1}\left\{-u^{n/(n-m+1)} + \left(\frac{1}{n-m+1} - \frac{1}{m-1}\right)u\right\}. \tag{16b}$$

This system is to be solved in $0 < \xi < \xi_b$ for appropriate m and n, subject to the boundary conditions derived from (13a, b), (14)

$$u'(0) = 0, \quad u(\xi_b) = 0. \tag{17a, b}$$

An additional condition is provided by Equation (11a), which in combination with (15a, b, c) may be rewritten in the form

$$\begin{aligned}\tilde{Q} &\equiv \dot{Q}L^{(n+1-m)/(m-1)} \\ &= (2\xi_b)^{(n+1-m)/(m-1)} \int_{-L/2}^{L/2} \left(\frac{u}{m-1} + u^{n/(n-m+1)} + \xi\frac{u'}{n-m+1}\right) \mathrm{d}\xi. \end{aligned}\tag{17c}$$

Equations (16)–(17) were solved numerically, for several values of the dimensionless oil-discharge parameter $\tilde{Q} = \dot{Q}L^{(n+1-m)/(m-1)}$ and parameters m and n, corresponding to the practically important situations of oil-water transport in aquifers (see Section 5). We used the standard Runge–Kutta numerical integration procedure of the 5th order. In addition we found a closed-form analytical solution for the special case $m = n/2 + 1$, which enables us to examine the influence of various physical parameters and to verify the numerical solution obtained in the special case.

4.1. Analytical solution for $m = n/2 + 1$

Assuming that m and n are related via $m = n/2 + 1$, we can rewrite (15a, b) in the form

$$S(\hat{x}, \hat{y}) = (u(\xi)/\hat{y})^{2/n}, \quad \xi = \hat{x}/\hat{y} \tag{18a, b}$$

and the system (16a, b) takes the form

$$\frac{2}{n}(u(1+\xi^2)) = g(\xi) - \xi u^2, \quad g' = -u^2. \tag{19a, b}$$

These equations are being solved in the region $0 < \xi < \xi_b$, subject to the boundary conditions (17a, b). Integration yields the following expression for g

$$g(\xi) = \frac{2}{n}\frac{u(1+\xi^2) - 2\lambda/n}{\xi}, \tag{20}$$

where λ is an integration constant which will be determined below.

Introduction of (20) into (19a) yields

$$u' = -\frac{u(\xi^2-1) + 2\lambda/n}{\xi(\xi^2+1)} - \frac{n\xi}{2(\xi^2+1)}u^2. \tag{21}$$

In order to integrate this equation, we apply the Ricatti transformation [10, p. 295]

$$u = \frac{2(\xi^2+1)}{n\xi}\frac{1}{w}\frac{\mathrm{d}w}{\mathrm{d}\xi}, \tag{22}$$

in terms of as yet unknown function $w(\xi)$. Introducing (22) into (21) we obtain the following linear ODE

$$w'' + \frac{2(\xi^2-1)}{\xi(\xi^2+1)}w' + \frac{\lambda}{(\xi^2+1)}w = 0. \tag{23}$$

Further, define a new variable $z(\xi)$

$$z = \frac{1}{2}\left(1-\sqrt{\frac{1}{\xi^2+1}}\right), \quad 0 < z < x_b < 1/2, \tag{24a}$$

where $z_b = z(\xi_b)$. Note that the inverse function $\xi(z)$ is given by

$$\xi = \frac{2\sqrt{z(1-z)}}{1-2z}. \tag{24b}$$

Introduction of (24a) into (23) then yields the hypergeometric equation

$$z(z-1)\frac{\mathrm{d}^2w}{\mathrm{d}z^2} + (\tfrac{1}{2}-z)\frac{\mathrm{d}w}{\mathrm{d}w} - \lambda w = 0, \tag{25}$$

which possesses the general solution

$$w(z) = C_1F_1(z) + C_2z^{3/2}F_2(z). \tag{26}$$

In the above

$$F_1(z) = F(-1-\sigma, -1+\sigma, -\tfrac{1}{2}, z), \quad F_2(z) = F(\tfrac{1}{2}-\sigma, \tfrac{1}{2}+\sigma, \tfrac{5}{2}, z) \tag{27a,b}$$

are expressed via the hypergeometric function [11, pp. 555–566] and $\sigma = \sqrt{1+\lambda}$, and C_1, C_2 are constants to be determined below.

Using the properties of the hypergeometric series, we rewrite (27a, b) in the following forms

$$F_1(z) = (1-2z)\cos\beta + 2\sigma\sqrt{z(1-z)}\sin\beta \tag{28a}$$

and

$$F_2(z) = -\frac{3z^{-(3/2)}}{8\lambda\sigma}(2\sigma\sqrt{z(1-z)}\cos\beta + (2z-1)\sin\beta), \tag{28b}$$

where

$$\beta = 2\sigma(\arcsin\sqrt{z} + \pi l), \quad l = 0, 1, 2, 3 \ldots . \tag{29}$$

Introduction of (28a, b) into (26) yields

$$w(z) \;=\; \sin\beta\left(2C_1\sigma\sqrt{z(1-z)} - \frac{3C_2(2z-1)}{8\lambda\sigma}\right)$$
$$+\cos\beta\left(C_1(1-2z) - \frac{3C_2}{4\lambda}\sqrt{z(1-z)}\right). \quad (30)$$

Substituting (24b) in (22), we obtain the following expression for $u(z)$

$$u(z) = \frac{1-2z}{n}\frac{1}{w}\frac{\mathrm{d}w}{\mathrm{d}z}. \quad (31)$$

Differentiation of (30) with respect to z yields the following expression

$$\frac{\mathrm{d}w}{\mathrm{d}z} = 2C_1\lambda\cos\beta + \frac{3C_2}{4\sigma}\sin\beta, \quad (32)$$

which combines with (30), (31) to yield the following solution for u

$$u(\xi(z)) = \frac{2\lambda}{n}\frac{(2z-1)(3\tan\beta - 8\sigma\lambda C)}{(2z-1)(3\tan\beta + 8\sigma\lambda C) + 2\sigma\sqrt{z(1-z)}(3-8\sigma\lambda C\tan\beta)}, \quad (33)$$

where $C = C_1/C_2$. Using (22) and (24a), we can express $\mathrm{d}u/\,\mathrm{d}\xi$ as

$$\frac{\mathrm{d}u}{\mathrm{d}\xi}(z) = -(2z-1)^2\sqrt{z(1-z)}\left(2\frac{(u+2u^2/n)}{2z-1} - \frac{n(2z-1)}{4}\frac{1}{w(z)}\frac{\mathrm{d}^2w}{\mathrm{d}z^2}\right), \quad (34)$$

wherein $\mathrm{d}^2w/\,\mathrm{d}z^2$ is obtained by differentiation of (32)

$$\frac{\mathrm{d}^2w}{\mathrm{d}z^2} = \frac{-2C_1\lambda\sigma\sin\beta + \frac{3}{4}C_2\cos\beta}{\sqrt{z(z-1)}}. \quad (35)$$

Introducing (34), (35) into (17a) and using (33), we obtain C in the form

$$C = \frac{3}{8\lambda\sqrt{1+\lambda}\tan(2\pi l\sqrt{1+\lambda})}, \quad l = 0, 1, 2, 3\ldots. \quad (36)$$

Substituting (36) in (33), we finally obtain

$$u(z) = \frac{2\lambda(2z-1)}{n}\frac{1}{2z-1+2\sqrt{1+\lambda}\sqrt{z(1-z)}\tan(2\sqrt{1+\lambda}\arcsin\sqrt{z})}. \quad (37)$$

This solution is independent of the integer l. The equation for the boundary ξ_b between the capillary zone and the finely dispersed oil zone can be obtained by means of (17b)

$$2\sqrt{1+\lambda}\arcsin\sqrt{z(\xi_b)} = \tfrac{1}{2}\pi. \quad (38a)$$

4.2. Calculation of Contamination Parameters

The inclination angle δ of the boundary is related to the boundary value ξ_b by $\xi_b = \tan\delta$. From (38a) it follows that

$$\delta = \frac{\pi}{2\sqrt{1+\lambda}}. \tag{38b}$$

Introduce (18a, b), into (10c) and use (19a, b) to obtain the expressions for the oil saturation flux

$$J_y = \hat{y}^{-2}\left(\frac{2}{n}(u\xi)' + u^2\right), \quad J_x = \hat{y}^{-2}\frac{2}{n}u'. \tag{39a,b}$$

The oil discharge $\dot{Q}$ at a distance $\hat{y}$ given by Equation (10c) is simplified using (17c), (18a, b), (39a) and the symmetry of u, thus yielding

$$\dot{Q} = 2\hat{y}^{-1}\int_0^{L/2}\left(\frac{2}{n}u\xi - g\right)\,\mathrm{d}\xi = -2\hat{y}^{-1}\left[\frac{u-2\lambda/n}{n\xi/2}\right]_0^{\xi_b}. \tag{40a}$$

It can be shown from Equations (17a) and (21) that

$$\frac{u-2\lambda/n}{n\xi/2} \to 0 \quad \text{as } \xi \to 0, \tag{40b}$$

which combines with (40a) written for $\hat{y} = \hat{y}_+$ and (15c) to obtain the following expression for the total discharge

$$\dot{Q} = \frac{16\lambda}{Ln^2}. \tag{41}$$

This yields the value of the yet unknown coefficient λ

$$\lambda = \frac{\dot{Q}Ln^2}{16} = \frac{\tilde{Q}n^2}{16}, \tag{42}$$

wherein for the specific relation between m and n the oil-discharge parameter, defined in (17c) reduces to $\tilde{Q} = \dot{Q}L$. According to the latter, $\tilde{Q}$ can be identified as the modified discharging capacity of the oil source. Introducing of (42) into (39b), we obtain

$$\delta = \frac{\pi}{2\sqrt{1+\tilde{Q}n^2/16}}. \tag{43}$$

We can show that the total oil discharge in the water-flow direction at any location $\hat{y} > \hat{y}_+$ is

$$\dot{Q}(\hat{y}) = \hat{y}^{-1} \frac{\tilde{Q}}{2 \tan \dfrac{\pi}{2\sqrt{1 + \tilde{Q}n^2/16}}}. \tag{44}$$

It may be seen that the total contaminant rate decays as $\hat{y}^{-1}$.

5. Results and discussion

The solutions calculated in the previous sections enable investigation of the steady-state contamination pattern in the aquifer. Two features of the oil distribution are important for environmental applications: the overall extension of the contamination plume and its shape. The former can be characterized by the polluted aquifer area, say the region where $S \geqslant 0{\cdot}2$. The shape of the plume can be described by the location of the boundary between the immiscible and dispersed zones (the zero saturation line, or its opening angle δ).

The oil is transported in the aquifer by oil advection and diffusion. The advection along the water flow direction (y-direction) is governed by the parameter n, appearing in the governing Equations (10a, b, c). This parameter reflects the effects of the oil/water relative permeabilities and mainly their viscosities (see Equations (7b, 8a)). Namely, smaller n correspond to faster advection (low viscosity oil). This may be inferred from Equations (10c), where the dimensionless) advection velocity is identified as $S^{n-1}(n > 1)$.

In addition to advection with the water flow, the oil also moves as a result of saturation gradient, from the more polluted to less polluted zones. This is perceived in Equations (10b, c) as diffusion, with the effective diffusivity S^{n-m} arising from oil penetration through the interstices under the influence of the capillary pressure gradient (see Equation (7c)). As such, the relative effect of the capillary diffusion is characterized by the difference $n - m$, namely when $n > m$ the diffusion is weak; when $n < m$, the opposite situation prevails, *i.e.*, the diffusion is strong. Physically the former case corresponds to the situation where the oil viscosity is much larger than that of water (n-large) and the pores are coarse (m-small) and do not favor capillary motion [2]. Mathematically, when $n > m$, the effective diffusivity vanishes at $S \to 0$, which means that near the boundary between the immiscible and dispersed zone the oil is mainly transported by advection. On the other hand, when $n < m$, the diffusivity indefinitely increases as S approaches zero. This points to the tendency of increasing the extension of the plume as $n - m$ becomes negative. As shown below, this tendency is combined with the influence of the oil discharge rate.

The above general observations are used to interpret the results obtained from the analytical model and numerical calculations. Figure 2 depicts the angle δ of the boundary between the immiscible and dispersed zone as a function of the dimensionless parameter $\tilde{Q} = \dot{Q}L = \dot{Q}^* L^* q F_0 \mu^2 / \gamma_{0w}^2 \Psi_0^2 \kappa_{xx} \kappa_{yy}$. This parameter measures the influence of both the total pollutant discharge rate $\dot{Q}$ and L as a single product. Therefore, at large distance $\hat{y}$ where our solution is valid, the contamination may be viewed as a result of a point source $(L \to 0)$ with infinite discharge rate $(\dot{Q} \to \infty)$. The curves depicted in this figure are obtained from the analytical solution, developed for $m = n/2 + 1$. Therefore, the different curves correspond to the diffusion parameter $n - m$ varying from $n - m = -\frac{1}{2}$ (for $n = 1$) to $n - m = 1$ (for $n = 4$). We can see that, in accordance with the trend generally outlined above, the widest opening angle of the singularity associated with infinite value of the diffusivity S^{n-m} is integrable, which results in a finite extension of the plume in the lateral (x-) direction (*i.e.*, $\delta < \pi/2$). When $n - m \leqslant -1, \delta = \pi/2$ and the plume lateral boundaries tend to infinity. Practically, in all physically meaningful cases, $n > 1$; hence $n - m > -\frac{1}{2}$, and for all nonzero water flow-rates the plume has a finite lateral extension.

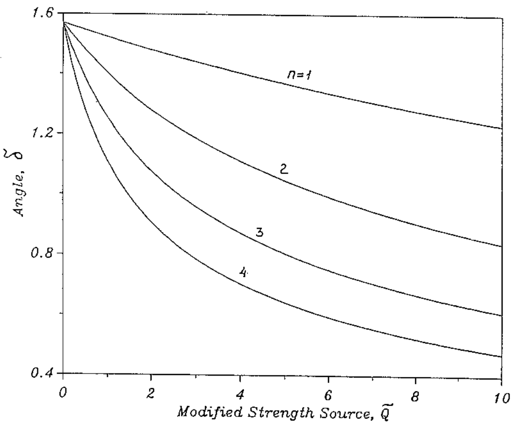

Figure 2. The angle δ describing the boundary between the immiscible and dispersed oil zone vs. oil strength parameter $\tilde{Q} = \dot{Q}L$.

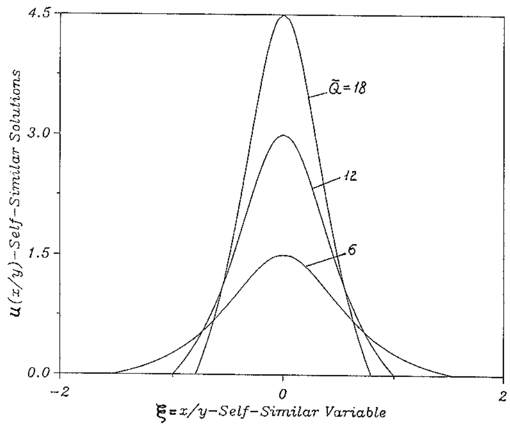

Figure 3. Self-similar solutions for the saturation distribution: $n = 2, m = 2$.

It can be observed that as the flow-rate parameter $\tilde{Q}$ decreases, the angle δ of the immiscible zone approaches $\frac{1}{2}\pi$. On the contrary, with increasing $\tilde{Q}, \delta$ diminishes, which reveals the important influence of oil advection in the water flow direction. With increasing water flow-rate this oil-transport mechanism becomes more significant, compared with the diffusion across the flow (in x-direction), induced by the capillary forces. This effect of the water flow-rate can also be observed in Figure 3, which depicts oil saturation profiles for three values of $\tilde{Q}$ and $n = m = 2$ (intermediate pore size and medium oil viscosity). Such curves may be useful for calibration of the model, which we can achieve by matching various self-similar profiles with oil-saturation data collected from observation wells in the aquifer.

Note that the different curves appearing in Figure 2 show the situations varying from discharge of a light (low-viscosity) oil into a coarse-grained aquifer $(n = 1, m = 1{\cdot}5)$ to discharge of a heavy (high-viscosity) oil into a fine-grained aquifer $(n = 4, m = 3)$.

The nonlinear advection effect of $\tilde{Q}$ on the downstream plume-like contamination pattern can be observed in Figures 4–6 (for $n = m = 2$). It can be seen that in addition to reducing the value of the opening angle δ, the effect of increasing $\tilde{Q}$ is to increase the downstream values of oil saturation. The contamination zone can be characterized by the location of one of the iso- saturation lines (say $S = 0{\cdot}2$), or its largest lateral and streamwise extensions. Figures 4–6 allow such evaluations on the basis of scales L_x, L_y (see Equations (9d, e)) calculated from the literature data, or from the results of model calibration.

We can see the influence of the parameters m, n on the saturation distribution by comparing the contamination patterns in Figures 4, 7. Increasing $m = n$ from 2 (see Figure 4) to

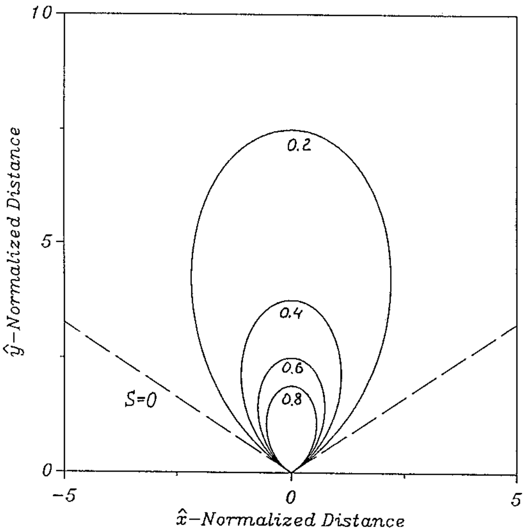

Figure 4. Distribution of the oil saturation: $\tilde{Q} = 6, n = 2, m = 2$.

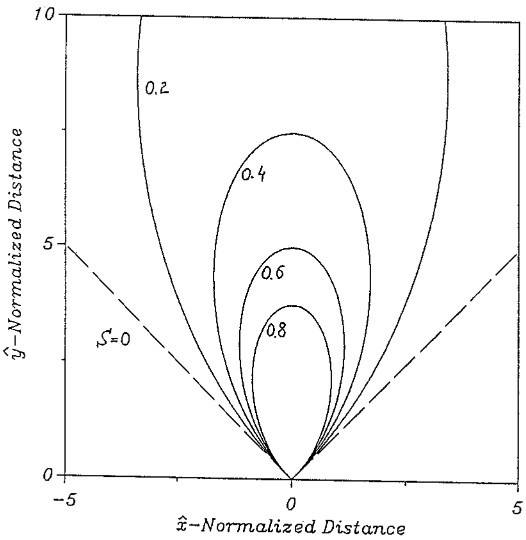

Figure 5. Distribution of the oil saturation: $\tilde{Q} = 12, n = 2, m = 2$.

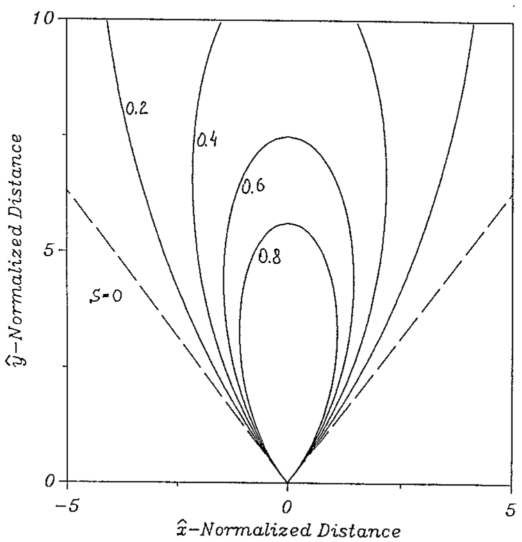

Figure 6. Distribution of the oil saturation: $\tilde{Q} = 18, n = 2, m = 2$.

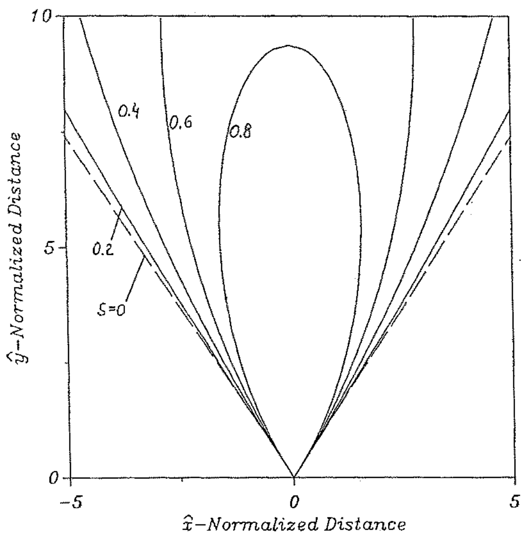

Figure 7. Distribution of the oil saturation: $\tilde{Q} = 6, n = 4, m = 3$.

$n = 4, m = 3$ (see Figure 7) leads to the contamination plume extended in the downstream direction. In this figure the factor $n - m = 1$, *i.e.* the oil diffusivity vanishes at the boundary between the immiscible and dispersion zones (*cf.* with constant diffusivity prevailing in the case shown in Figure 4). As such, oil advection is dominant in Figure 7 corresponding to the aquifer with larger pores than in Figure 4 plotted for smaller pores. Accordingly, larger values of n (larger pores) result in a plume more extended in the flow direction. This effect is,

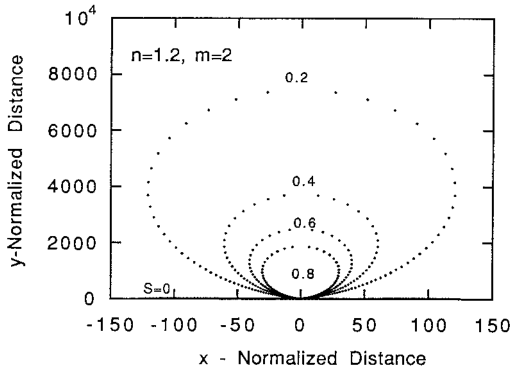

Figure 8. Distribution of the oil saturation: $\tilde{Q} = 6, n = 1{\cdot}2, m = 2$.

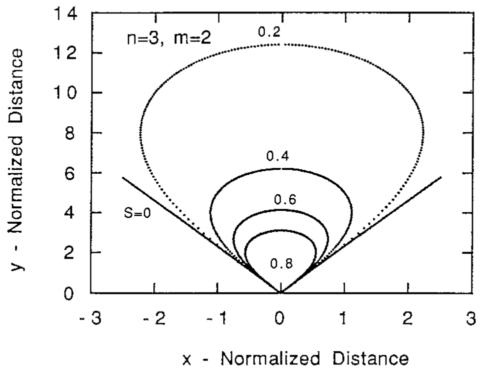

Figure 9. Distribution of the oil saturation: $\tilde{Q} = 6, n = 3, m = 2$.

however, lumped with the influence of the oil viscosity, which also changes with m. Namely, Figure 7 depicts contamination pattern of a more viscous oil than that shown in Figure 4.

In contrast with the above data, Figures 8–10 allow to elucidate the sole effects of (i) the oil-water viscosities and (ii) the pore size of the aquifer, as embodied within the parameters n and m. These calculations were done for several cases where n and m were chosen independently. The data shown in these figures were obtained by numerical integration of Equations (16)–(17), since for these values of m and n no analytical solution exists.

Figures 8, 9 show the effect of the oil viscosity (as embodied within n) for fixed $m = 2$, corresponding for pore size index of $\lambda \sim 3$–4, (coarse sands or slit loam [2, 12]). Figure 8 shows the plume form when the viscosity of oil is much lower than the viscosity of water (*i.e.*, very light oil [13]). On the other hand, Figure 9 shows the opposite situation, where the oil viscosity is larger than that of water (heavy oil). We can see that the plume extension of the low viscosity oil is much larger than that of the more viscous oil: the difference of the plume sizes in the flow direction amounts to a factor of 1000. This is clearly attributed to the dominating influence of the oil diffusion (capillary dispersion). Mathematically this may be seen from the power $n - m = -0{\cdot}8$ of the S- dependence of the oil diffusivity in Figure 8. In this case the plume opening contamination angle is very close to $\frac{1}{2}\pi$ and the dimensionless extension of the line $S = 0{\cdot}2$ reaches several thousands. This implies that from the point of view of environmental contamination the latter case is more dangerous, than the advection-dominated pattern.

The effect of the pore structure for the viscosity ratio $\mu_o/\mu_w \sim 10$ (high-viscosity oil) can be elucidated from Figures 9, 10. The decreasing pore size (increasing m) causes extension of the plume in both x- and y-directions, by promoting the oil capillary diffusion. Mathematically this can be rationalized by observing that the oil diffusivity is larger in circumstances depicted the Figure 9 than in Figure 8.

Below we estimate the characteristic dimensions of the pollution zone, as obtained from the similarity solution for water-oil mixture ($\mu_w = 10^{-3}$ kg/ms, $\gamma_{ow} = 0{\cdot}03$ N/m). For water velocity 0·01 m/day in a coarse sand aquifer with capillary pressure of 2 cm H_2O and permeability of 10^{-8} cm^2 one obtains from (9e) the characteristic length $L_y = 1{\cdot}7$ m and the characteristic time scale given by (9c) $T \sim 50$ days. Taking $L^* = 1$ m as a characteristic extension of the oil leakage source, $F_0 \sim 1$, the leakage rate $\dot{Q}^* = 0{\cdot}36\,\mathrm{m}^3$ per day which

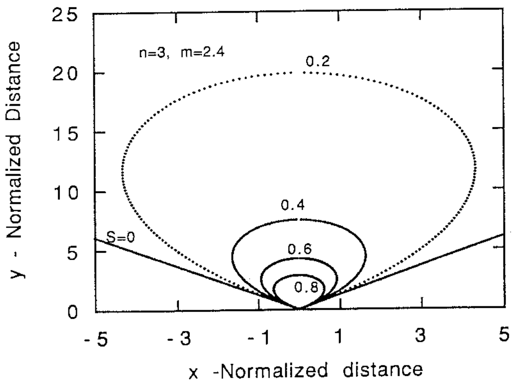

Figure 10. Distribution of the oil saturation: $\tilde{Q} = 6, n = 3, m = 2{\cdot}4$.

corresponds to the data of Figure 5, one obtains that the extension of the plume calculated in Figure 5 is about (10–20) $L_y \sim$ 17–34 m. Moreover, the time in which the steady oil distribution is achieved $t \gg 50$ days, *i.e.* about 0·5–1 year. These estimates are generally confirmed by several field studies [14].

6. Summary and conclusions

The distribution of immiscible oil contaminant in a saturated porous medium is analyzed and described by basic two-dimensional equations of two-phase flow. The self-similar solution obtained here pertains to the steady-state oil transport. The influences of the leakage rate from an oil source and its length are lumped in a single parameter $\tilde{Q} = \dot{Q}L$, describing the source capacity. It is found that increasing $\tilde{Q}$ reduces the value of the immiscible zone angle δ and increases the downstream oil saturation.

We have studied the effects of oil-water mixture properties and the aquifer porous structure, as embodied within parameters m and n, appearing in the governing equations. Contamination pattern of low-viscosity oils in aquifers with coarse porous structure is characterized by a plume extending mainly in the water-flow direction, rather than in the lateral direction. Highly viscous heavy oils discharging into the aquifer with fine pores have a tendency to spread sidewards.

Acknowledgment

This research has been supported by the Technion V. P. R. Fund – B. and I. Green Research Fund. The authors are grateful to Dr. B. Skachek for performing computations of the contamination patterns in Figures 8–10.

References

1. L. M. Abriola, Mathematical modeling of the multiphase migration of organic compounds in a porous medium, Ph. D thesis, Princeton Univ., Princeton, N. J. (1983) 412pp.
2. A. Pistiner, M. Shapiro and H. Rubin, Similarity solutions for immiscible phase migration in porous media: An analysis of free boundaries. *Transp. Porous Media* 5 (1990) 491–515.
3. J. Bear, *Dynamics of Fluids in Porous Media*. New York: Dover (1988) 764pp.
4. J. J. Fried, P. Muntzer, and L. Zilliox, Ground-water pollution by transfer of oil hydrocarbons. *Ground Water* 17 (1979) 586–595.

5. L. A. Spielman and Y. P. Su, Coalescence of oil in water suspensions by flow through porous media. *Ind. Eng. Chem. Fundam.* 16 (1977) 272–282.
6. L. A. Spielman and S. L. Goren, Theory of coalescence by flow through porous media. *Ind. Eng. Chem. Fundam.* 1 (1972) 66–73.
7. G. F. Pinder and L. M. Abriola, On the simulation of nonaqueous phase organic compounds in subsurface. *Water Resour. Res.* 22 (1986) 109s–119s.
8. T. S. Ramakrishnan, D. Wilkinson and M. Dias, Effect of capillary pressure on the approach to residual saturation. *Transp. Porous Media* 3 (1988) 51–79.
9. H. Soo and C. J. Radke, Filtration model for the flow of dilute stable emulsions in porous media. *Chem. Eng. Sci.* 41 (1986) 263–272.
10. E. Kamke, *Handbook on Ordinary Differential Equations.* Moscow: Nauka (1971) 576pp.
11. M. Abramowitz and I. A. Stegun, *Handbook of Mathematical Functions.* New York: Dover (1970) 1046pp.
12. L. G. King, *Imbibition of fluids by porous solids*. Ph. D. Thesis, Colorado State University, Fort Collins (1964) 472pp.
13. S. J. Pirson, *Oil Reservoir Engineering*. New York: Mac-Graw Hill (1958) 735pp.
14. S.M. Testa and D. L. Winegardner, *Restoration of Petroleum Contaminated Aquifers*. Chelsea: Lewis Publishers (1991) 269pp.